Ayman Mohammed Ibrahim, Imran Mohd Ibrahim, Noor Azwan Shairi

Centre for Telecommunication Research and Innovation (CeTRI), Fakulti Kejuruteraan Elektronik dan Kejuruteraan Komputer (FKEKK),
Universiti Teknikal Malaysia Melaka (UTeM), Melaka, Malaysia

Compact V-Shaped MIMO Antenna for LTE and 5G Applications

Abstract. A compact sierpinski MIMO antenna was designed in the bands of 4.4 - 4.9 GHz and 5.15 - 5.925 GHz.The proposed dimension of the antenna were 21 × 24 × 0.8 mm, and was fabricated with inexpensive FR4 substrate with a thickness of 0.8 mm, a dielectric constant of 4.3, and 0.035-mm thick copper lining. The fabrication and measurement outcomes derived from the MIMO prototypes revealed that the proposed MIMO antennas are better in terms of size, isolation and the ECC. These attributes are suitable for LTE and 5G smartphone applications, which are being introduced into Chinese and Japanese markets.

Streszczenie. Przedstawiono projekt anteny MIMO o paśmie 4.4 – 4.9 GHz oraz 5.13 – 5.925 GHz. Wymiary anteny: 21 × 24 × 0.8 mm. Badania wykonanej anteny wykazay jej przydatność do LTE i 5 G zastosowań. (Kompaktowa antena MIMO dla zastosowań LTE i 5G)

Keywords: *5G band, Envelope correlation coefficient (ECC), Fractal antenna, Isolation, LTE, MIMO antenna.*
Słowa kluczowe: Pasmo 5G, antena MIMO, LTE

Introduction

Over the past three decades, improvements in cellular communications standards have dramatically altered the construction of antennas. Two main parts are included in this development. First, it is the interest of users, which consists mainly of ergonomic and aesthetic considerations, and secondly, the introduction of different spectra in line with evolving regulatory standards. Antenna design is one of the many difficult requirements for mobile system designers. The rapid growth of mobile wireless systems requires about 5G multi-band, broadband, or even broadband antennas to cover the interoperability of mobile services and reduce system complexity[1]–[5].

At the same time, antennas are needed to be placed closer to each other as there is a constraint of space as well. As the antennas are placed closer to each other, the near field effect dominates in the form of surface and space waves, giving rise to strong mutual coupling among the antennas. This causes a decrement in antenna efficiency, bandwidth, and gain. The existence of mutual coupling degrades the maximum achievable performance of the communication system. Besides, the design of MIMO antennas over a limited space requires various approaches for the reduction of mutual coupling, otherwise the gain, efficiency, diversity gain and radiation patterns would be severely affected 6; Malviya, Panigrahi, and Kartikeyan, 2017). Thus, the mutual coupling reduction techniques should be applied with greater care, and other parameters must be considered. One of the possible solution to the problem of mutual coupling is the use of isolation techniques. The isolation decreases the mutual coupling among antenna elements and improve the gain and efficiency of the system (Chouhan, 2017)[6]–[10]. As such, this paper attempted to solve the above-mentioned issues with a high isolation printed on two-element arrays operating in the centre frequencies of 4.65 GHz and 5.5375 GHz in the bands of (4.4-4.9) and (5.15-5.925) GHz

Antenna Design and Analysis

There are many types of Sierpinski fractal for example sierpinski poly-flake, sierpinski hexagon, sierpinski pentagon, sierpinski square, sierpinski maze, sierpinski carpet, sierpinski curve, sierpinski arrowhead curve and sierpinski gasket. One of the most widely used structures in fractal antennas is Sierpinski gasket, which consists of equal dimension triangles. There are two methods to build the structure, either by decomposition method or by a multiple copy method[11]. The second method was used to design the fractal antenna in this paper. Fig.1 represents this method.
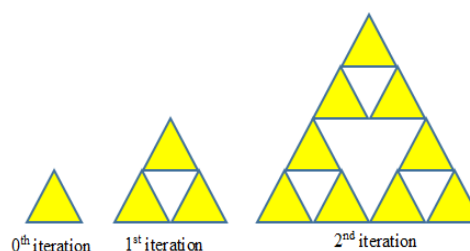

Fig.1: Multiple copy approach of sierpinski gasket arrangement

During 1st iteration, the structure was made with three copies of same triangle from the 0th iteration, with two triangles at the bottom and the third one on top of these two triangles. In the 2nd iteration, the same process was repeated, but with the whole structure formed by three triangles in the 1st iteration. So the dimensions of the next iteration increased by a factor of 3 as compared to the dimensions in the previous iteration. The above transformation of the triangles in order to generate any order of iterations, has been represented by a mathematical formula in Equation (1)[12].

$$(1) \qquad Q\begin{pmatrix} X \\ Y \end{pmatrix} = \begin{pmatrix} r\cos\theta & -s\cos\phi \\ r\sin\theta & s\sin\phi \end{pmatrix}\begin{pmatrix} X \\ Y \end{pmatrix} + \begin{pmatrix} X_0 \\ Y_0 \end{pmatrix}$$

where, r and s are scaling factors, θ and ϕ are rotation angles and X0 and Y0 are the amounts of transformation. If, the scaling factors r and s, are either reduction or magnification, the transformation process is self-affine, but if r = s and $\theta = \phi$, the transformation process is self-similar. The design of proposed fractal printed monopole antenna was started with a V-shaped initiator, which consisted of a radiating patch with overall dimensions of 7 mm × 8 mm, printed on a substrate with dimensions of Wp mm × Lt mm, fixed on the FR4 material with a dielectric constant of 4.3 and a copper lining thickness of h = 0.8 mm. The antenna was fed through a microstrip line with a length of Lf mm and a width of Wf mm, designed specifically for 50 Ω. On the other side of the substrate, a ground plane was printed with dimensions of 6.8 mm × 8.0 mm. The gap between the rectangular patch and the ground plane was g1 = 1.2 mm. The geometry of the reference antenna is shown in Fig. 2 3.9 (a) and the geometry of the V-shaped initiator antenna is shown in Fig.2 (b). The resonant frequency was calculated by using Equation (2):

$$(2) \qquad f_r = \frac{c}{2L\sqrt{\epsilon_r}}$$

The initiator in the new proposed fractal antenna is a rectangular patch, as shown in Fig. 2 (a). The arms of the patch were equal in dimensions, x+1 = y = 8, in 0th iteration, as shown in Fig2. (b). In 1st iteration, a mutated rectangular patch, with half of the size of the one used in the previous stage, was added to the shape of fractal antenna. If the x-axis is the bottom of the left modified patch and y-axis passes through the center of the left modified patch in Fig. 2 (e), Q1 was configured by adding the half sized modified patch to both the left and right sides of MIMO antenna, as shown in Fig. 2 (e). The red line mentioned in Fig. 2 (e), lies on y-axis and passes through the center (black points) of all the transformation structures (Q1, Q2, Q3). Hence, the scaling factors became r = s = 0.5, the rotation angles became $\theta = \phi = 0$ and the transformation factors became X0 = 0, Y0 = 2.5), as shown in Equation (3)

(3) $$Q_1 \begin{pmatrix} X \\ Y \end{pmatrix} = \begin{pmatrix} 0.5 & 0.5 \\ 0 & 0 \end{pmatrix} \begin{pmatrix} X \\ Y \end{pmatrix} + \begin{pmatrix} 0 \\ 2.5 \end{pmatrix}$$

While Q2 was made by adding a quarter sized modified patch to the structure with scaling factors, r = s = 0.25, zero rotation angles and the transformation factors, X0 = 0 and Y0 = 3.75 as mentioned in Equation (4):

(4) $$Q_2 \begin{pmatrix} X \\ Y \end{pmatrix} = \begin{pmatrix} 0.25 & 0.25 \\ 0 & 0 \end{pmatrix} \begin{pmatrix} X \\ Y \end{pmatrix} + \begin{pmatrix} 0 \\ 3.75 \end{pmatrix}$$

Finally, for Q3, the scale factors were r = s = 0.125 and the transformation factors were X0 = 0 and Y0 = 4.375 as shown in Equation (5):

(5) $$Q_3 \begin{pmatrix} X \\ Y \end{pmatrix} = \begin{pmatrix} 0.125 & 0.125 \\ 0 & 0 \end{pmatrix} \begin{pmatrix} X \\ Y \end{pmatrix} + \begin{pmatrix} 0 \\ 4.375 \end{pmatrix}$$
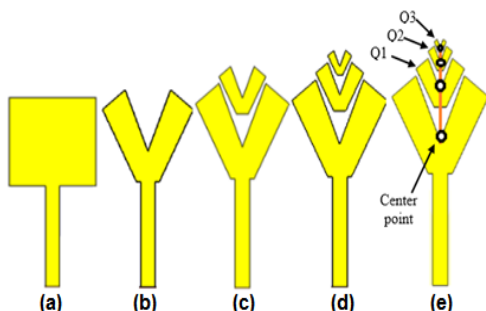

Fig. 2: Cell configuration process for V- shaped antenna,(a) Rectangular patch, (b) 0th iteration, (c) 1st iteration, (d) 2nd iteration, and (e) 3rd iteration

The total length of the upper arm in Fig. 3 was calculated as m2 + m2 +m9 + m9 = 15.16 mm with the length of right arm as m1 = 6.26 mm and the length of left arm as m1 = 6.26 mm. The length of lower arm was calculated as m13 + Wf + m13 = 2.01mm. If the perimeter of the modified rectangular patch is P1 and the perimeter of 1st iteration is P2, then P4 can be calculated using Equation (6):

(6) $$P_4 = \frac{1}{2} P_3 = \frac{1}{4} P_2 = \frac{1}{8} P_1$$

The perimeter of cascade modified patches, Pci at each iteration can be calculated using Equation (7):

(7) $$P_4 = \frac{1}{2} Pc_{i-1} \quad i = 1, 2, 3 \text{ and } 4$$

The term (2L) in equation (2) represents half perimeter of the rectangular patch, so equation (2) can be rewritten as:

(8) $$f_r = \frac{c}{P\sqrt{\varepsilon_r}}$$

However according to [12];

(9) $$\frac{the\ perimeter\ of\ modified\ patch}{the\ perimeter\ of\ rectangular\ patch} = \frac{29.69}{30} = 0.9896$$

Equation (8) can be written as Equation (10):

(10) $$f_i = \frac{c}{0.9894 P_i \sqrt{\varepsilon_r}}$$

Let's suppose, $\frac{c}{\sqrt{\varepsilon_r}}$ =K, the Equation (10) will be written as Equation (11):

(11) $$f_i = \frac{K}{0.9896 Pc_i}$$
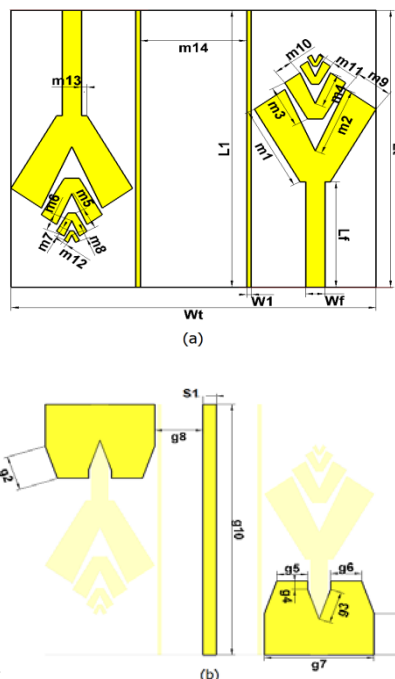

Fig. 3: Proposed design geometry of fractal V- shaped MIMO antenna (a) Front view (b) Back view

Table 1: Parameters and dimensions of the fractal Siperpinki MIMO antenna

parameter	value	parameter	value	parameter	value
Lf	8	m5	1.57	m12	0.31
Wf	1.27	m6	1.27	m13	0.37
W1	1	m7	0.78	m14	7
m1	6.26	m8	0.63	g1	3.5
m2	5.08	m9	2.5	g2	2.85
m3	3.13	m10	1.25	g3	2.68
m4	2.54	m11	0.63	g4	0.7
g5	2.27	g6	2.27	g7	8
g8	3.5	S1	3	g10	21
L1	21	Lt	21	Wt	24

Table 1 displays the dimensions of the proposed MIMO antenna. Each radiating element of the two-element MIMO antenna held a symmetrical monopole antenna fed with a 50 Ω microstrip line. The proposed MIMO antenna included two separate ports with a distance of 7 mm, monopoles printed on a 24 × 21 mm FR-4 substrate, as exhibited in Fig.4. For high isolation, neutralization lines were inserted between the two separate antennas of the patch plane and using defected ground structure to the insert the slot in the ground plane. This procedure complemented the two vertical lines of the patch plane, with a width of W1 = 3 mm and length of L1 = 21 mm, a vertical with a width of g9 = 1 mm and length of g10 = 21 mm on the ground plane, and a slot with a length of g4+g3 = 3.38 mm, as shown in Fig.4.

Antenna Parametric analysis and optimization

The computer simulation reflection coefficient was used to study the effects of varying the dimensions of the radiating elements V1, V2, V3, V4, width of the gap g, width of center line S1 and length of ground line D.

1. Effect of the V1, V2, V3 and V4

From the equation 3.26, for the transform function V2, the scale factor (r = s = 0.5), the rotation angles ($\theta = \phi = 0$) and translation factors (x0 = 0, y0 = 2.5). Next, in equation 3.27, the values of scale factor (r = s = 0.25), the rotation angles ($\theta = \phi = 0$), and values of translation factor (x0 = 0, y0 = 2.92) for the transformed structure V3. According to equation 3.28, the values of scale factor (r = s = 0.125), the rotation angle ($\theta = \phi = 0$) and translation factors (x0 = 0, y0 = 3.23) for the transformed structure V4. The first iteration was formed by the integration of two modified patch antenna, each is fed by symmetrical strip lines F1 and F2. The next iteration was made by adding the half size of the modified patch to antenna-1 to configure antenna-2, as shown in Fig. 3. The same procedure was applied in the 3rd iteration except that the additional modified patch had one-fourth size of the original one, while the fourth iteration was one-eighth of the original one. In order to illustrate the effect of the structures on the production of operating bands, the proposed antenna was simulated by adding a V-shape to the patch plane. The simulated results to the first and fourth iterations are shown in Fig. 5. The difference in results suggests the influence of adding a V-shaped structure, to generate various LTE and 5G bands.
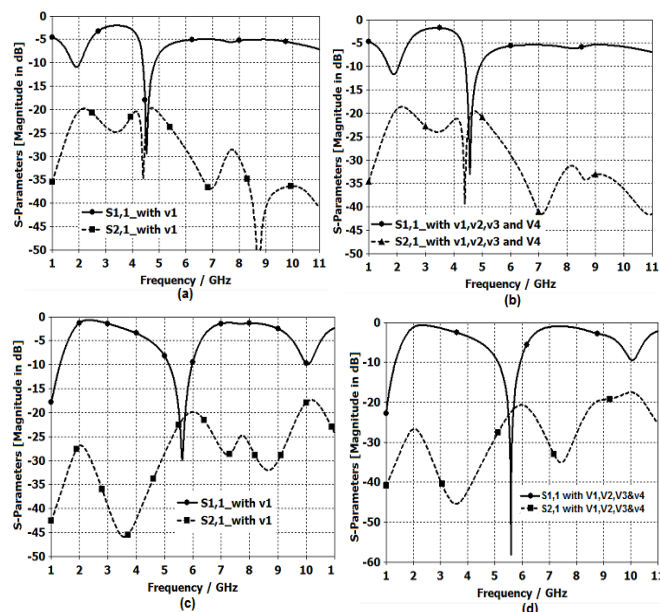

Fig. 5: Simulated reflection coefficients and transmission coefficients of the sierpinski MIMO antenna of (a) 1st iteration at S1 = 3.35 mm (b) 4th iteration at S1 = 3.35 mm (c) 1st iteration at S1 = 4.3 mm and (d) 4th iteration at S1 = 4.3 mm.

By fixing the other radiation elements and changing the width of the centre line, the results of the proposed design changed. In first iteration, the solid curve presents the return losses of the antenna when the width of the centre line S1 was 3.35 mm. Only one operating band (4.4 - 4.85 GHz) was observed with a return loss of -29.5 dB and the isolation value of -19.75 dB as shown in Fig. 5 (a).The Fig. 5 (b) presents the fourth iteration, when the width of the center line was S1 = 3.35 mm, the resulting operating band was 4.4 - 4.8 GHz with a return loss of -33 dB and the isolation value of -19 dB, as shown in Fig. 5 (b).

By changing the width of the centre line S1 = 4.3 mm with first iteration, the simulations showed a single operating band (5.12 - 5.97 GHz) with a return loss of -30 dB and the isolation value of -20 dB, as shown in Fig. 5 (c). When using the fourth iteration, the operating band was changed to 5.15 - 5.925 GHz, isolation was dropped to -21 dB with the return losses of -58dB, as shown in Fig. 5 (d).

2. Effect of length of ground line D

Fig.6 shows the effect of varying the size of the ground line on the bandwidth and isolation of the proposed fractal MIMO antenna. Given that modifying the ground dimensions can change the antenna band and the isolation factor between two antenna elements, the dimensions of the ground plate can be modified to select the operating band. When the dimension of the ground plate was set to 8 × 3.8 mm2, the operating band was shifted to 100 MHz with the isolation of -15.5dB, as indicated by the solid black curve in Fig. 6. The blue curve in Fig. 6 represents the value of return losses when the dimension of the ground plate was 8 × 6.26 mm2, the band shifts to 200 MHz, while the isolation was increased to -16.5 dB.
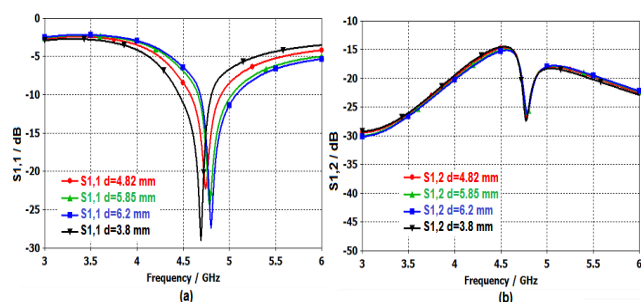

Fig. 6: S-parameters of the fractal sierpinski MIMO antenna with changing values of the ground line while fixing other parameters. (a) Simulated return loss (b) Simulated isolation.

3. Effect of width of center line S1

The parametric study showed that the width of operating band and the isolation of the MIMO antenna are highly sensitive to variation in the width of center line S1. The same was found true from simulation results, as shown in Fig. 7. This is because the increase or decrease in the width of center line S1 values was found to have induced a change in the resonant frequency of the design bandwidth and isolation between the port elements. The isolation of different adjacent antennas that are resulted from a change of the width of center line S1, are thus illustrated in Fig. 7. As shown in Fig.7, when the width of S1 was 4.3 mm, the peak isolation, obtained in the operating band 5.15 - 5.925 GHz, was -20 dB. But, when the width of S1was changed to 0.2 mm, isolation obtained in the operating band 4.4 - 4.9 GHz was -19.5 dB.

Effect of width of the gap g: The parametric study showed that the frequency response and bandwidth of the MIMO antenna are highly sensitive to variation in the gap width (g). The same was found true from simulation results, as shown in Fig. 8. On the other hand, the gap width does not effect isolation between antenna elements, as shown in Fig.8.

In summary, the design of proposed fractal sierpinski MIMO antenna demonstrates two key points. Firstly, the self-similarity property of the fractal shape was used to construct the structure of the multi-frequency antenna to achieve the required band. For this, fractal geometries were applied to the first iteration of the V-shaped structure, and the resonance elements, which were scaled-down copies of the original element, were added to the top edges of the shape, as illustrated in Fig. 4. The return loss response

profile shows that the matching in the bands (4.4 - 4.9 GHz and 5.15 - 5.925 GHz) was good. Secondly, the effect of changing the dimensions or the location of some important parts in the MIMO antenna structure proves that optimum dimensions. location of the proposed MIMO antenna must match the optimum values. These optimum values are colored in green in Table 2, that helped in achieving the required frequency spectrum for both LTE and 5G applications.
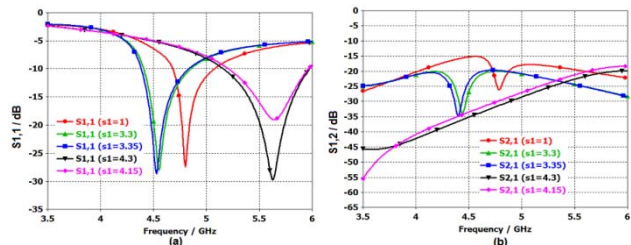

Fig. 7: S-parameters of the fractal sierpinski MIMO antenna with changing values of the S1 while fixing other parameters. (a) Simulated return loss (b) Simulated isolation.
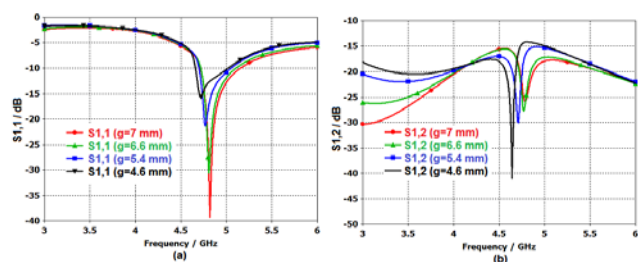

Fig. 8: S-parameters of the fractal sierpinski MIMO antenna with changing values of the gap g while fixing other parameters. (a) Simulated return loss (b) Simulated isolation.

Table 2: Optimum dimensions of the proposed fractal sierpinski MIMO antenna

Parameters (mm)	BW. GHz	Isolation dB	State
Gap g=7, D=4.82, 1=4.3, with v1-v4	5.15-5.925	-21	optimum
Gap g=7, D=4.82, s1=3.35, with v1-v3	4.4-4.8	-19	optimum
Gap g=7, D=4.82, s1=4.3, with v1	5.12-5.97	-20	Not useful
Gap g=7, D=4.82, s1=3.35, with v1	4.4-4.85	-19.75	Not useful
Gap g=7, D=4.82, s1=0.4, with v1-v4	4.5722-4.887	-15.5	Not useful
Gap g=7, D=5.85, s1=0.4, with v1-v4	4.67-5	-16	Not useful
Gap g=7, D=6.26, s1=0.4, with v1-v4	4.78-5.06	-17	Not useful
Gap g=7, D=3.8, s1=0.4, with v1-v4	4.66-5.01	-16.5	Not useful
Gap g=7, D=4.82, s1=1, with v1-v4	4.68-5.07	-17.3	Not useful
Gap g=7, D=4.82, s1=0.2, with v1-v4	4.4-4.88	-20	Not useful
Gap g=7, D=4.82, s1=0.2, with v1-v4	4.4-4.9	-19.5	optimum
Gap g=7, D=4.82, s1=1, with v1-v4	5.21-6	-18.4	Not useful
Gap g=7, D=4.82, s1=3.35, with v1-v4	5.15-5.925	-20	optimum

Performances MIMO antenna
1. Isolation technique
As mentioned earlier, adoption of the hybrid techniques (NL with DGS) for the proposed antenna structure increases the isolation between the elements. To scrutinize the effect of this hybrid technique on the coupling reduction, Fig.9 (a) shows MIMO antenna with and without this technique, when S1 parameter is set at 4.3 mm. As can be seen in the Fig.9, existence of the isolation technique decreased the bandwidth at lower frequency edge to about 2.667 GHz. However, noticeable effect was seen on S21 curve; that is, the isolation between the elements. As can be seen, by the addition of hybrid technique, significant reduction was obtained in S21 curve. Fig. 9 (b), shows MIMO antenna with and without hybrid technique, when S1 parameter is set at 3.35 mm. As shown, the existence of the hybrid technique increased the isolation and decreased the bandwidth at lower frequency edge to about 1.663 GHz.
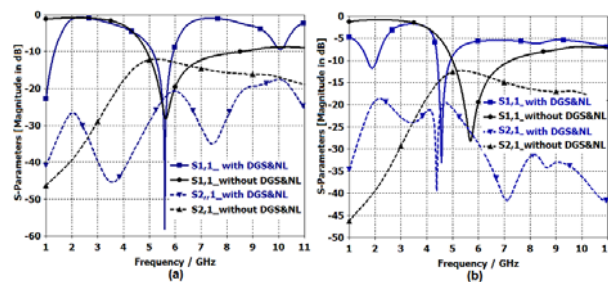

Fig. 9: A comparison with/without isolation technique of the fractal sierpinski MIMO antenna.(a) When parameter S1 = 4.3 mm (b) When parameter S1 = 3.35 mm

As it was stated already, the width of the S1 highly influences the isolation between elements, it was expected that any changes in the S1 parameter would influence the performance of proposed MIMO antenna. The effect of changing the length of S1, from 4.3 mm to 3.35 mm with a step of around 1 mm, is shown in Fig. 9 (b). As it is clearly seen, the best bandwidth and highest isolation was achieved when S1= 4.3 mm and 3.35 mm. Moreover, the surface current distribution, shown in Fig. 10, confirms the obtained results. In the first antenna, when rectangular slot with triangular base was embedded from the top edge of the ground plane, the surface current was mostly concentrated around the slots in opposite directions. The opposite alignment of the current around the embedded slots realized the notched functionality. Similar behaviour was also observed for the second antenna.
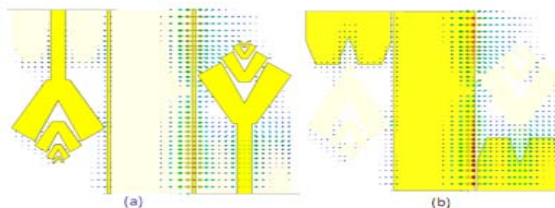

Fig. 10: Simulated current densities with port-1 of the sierpinski MIMO antenna of (a) Front (b) Back view

2. ECC and Efficiency
The simulation result of the ECC obtained was 0.006 and 0.00 for the two bands (4.4 - 4.9 GHz and 5.15 - 5.925 GHz) when changing S1. Apart from this, the proposed antenna achieved a higher level of efficiency, 50 – 57%, and 56 - 67% on 4.4 - 4.9 GHz and 5.15 - 5.925 GHz operating bands, respectively. The antenna efficiency was observed to be above 50% in all operating bands, as shown in Fig. 11.
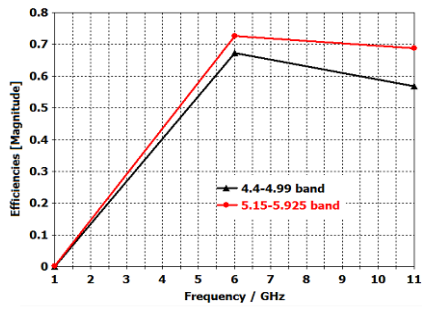
Fig. 11: Efficiencies of the fractal sierpinski MIMO antenna.

Prototype and Measurement result

The antenna prototypes were fabricated for the 4.4 - 4.9 GHz and 5.15-5.925 GHz bands with an operating frequency of 4.5 GHz and 5.5 GHz respectively, from an inexpensive FR4 dielectric and with overall dimensions of 21 × 24 × 0.8 mm3, as shown in Fig. 12. The simulated and measured reflection and transmission coefficients, demonstrated by the two representative antennas, were implied to have a similar level of performance, the antenna prototypes have shown measured isolation -22 dB and -20 dB at operating frequency bands, as shown in Fig. 13 (a) and Fig. 13 (c). Further, suitable agreement in gain was observed between simulated data (the solid) and the measured data (the dashed), as shown in Fig. 13 (b) and Fig. 13 (d).
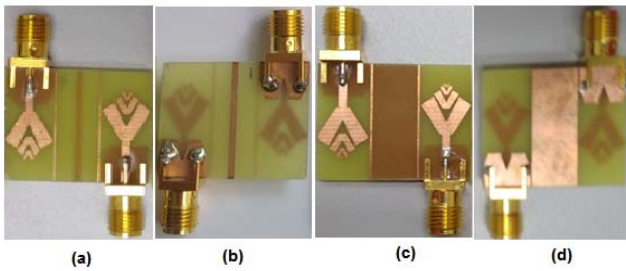

Fig. 12: A photograph of the fabricated fractal sierpinski MIMO antenna (a) Front view at band (5.15-5.2925) GHz (b) Back view at band (5.15-5.2925) GHz (c) Front view at band (4.4-4.9) GHz (d) Back view at band (4.4-4.9) GHz.
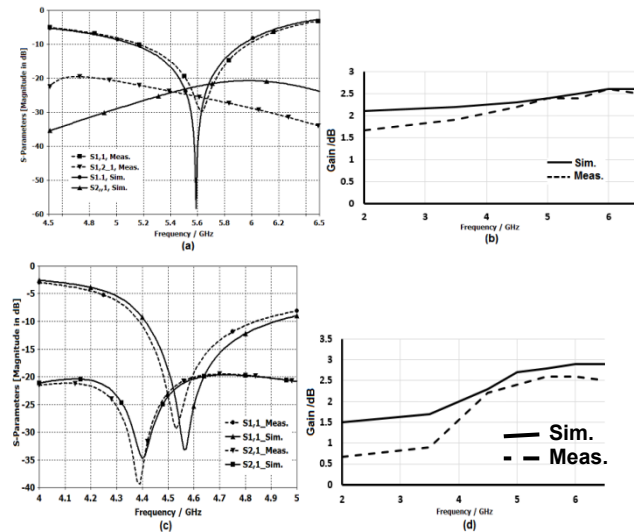

Fig. 13: Simulated and measured of the fractal sierpinski MIMO antenna of port 1 (a) S-parameters when band (5.15-5.925) GHz (b) Gain when band (5.15-5.925) (c) S-parameters when band (4.4-4.9) GHz. (d) Gain when band (4.4-4.9) GHz.

Further, Fig. 14 shown the results of the proposed MIMO antenna in both simulated and prototypes environment are compatible and confirm the existence of lower ECC between the two adjacent antenna elements. Also, the Measured and simulated S-parameters demonstrated by the two representative MIMO antenna in Fig. 15, were therefore implied to have a similar level of performance.
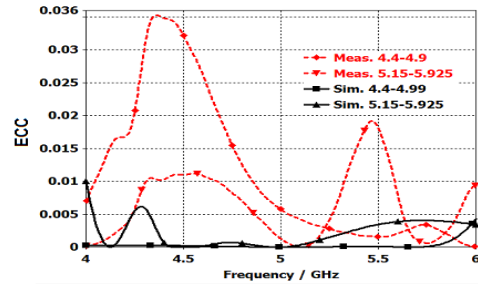

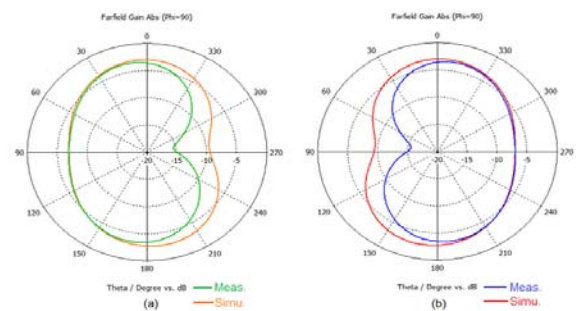Fig. 14: Simulated and measured ECC of the sierpinski MIMO antenna when 4.4-4.99 GHz and 5.15-5.925 GHz bands

Fig. 15: Normalized simulated and measured gain of the proposed siperpinki fractal MIMO antenna at operating frequency 4.5GHz (a) Gain of port1 (b) Gain of port2

Validation of the Proposed Antenna

Table 3 shows, the comparison of findings between this research works with other research work. The proposed antenna is compared with several selected types of research. The comparison was based on important characteristics, such as a number of ports, isolation, efficiency, envelope correlation coefficient, material, bandwidth and size. This V-shaped MIMO antenna is the best for LTE and 5G communications propose for several reasons.

Table 3: Comparisons between the proposed of MIMO antennas and previous related antennas

Ref.	BW (GHz),	Size (mm²)	Isolation	ECC	Efficiency (%)
[7]	4.4 - 4.99	31 × 31	< -20	< 0.002	(56 - 59)
[8]	3.7 - 4.2	26 × 46	< -20	< 0.0056	(78 - 87)
[3]	4.7 - 5	24 × 21	< -18.5	< 0.016	> 70
[13]	5.1 - 6	40 × 60	< -20	< 0.1	(70 - 81)
[14]	5.6 - 5.95	56 × 38	< -25	< 0.002	> 95
[15]	5.6 - 5.93	137 × 77	< -18	< 0.05	> 73
[16]	3.4 - 3.8	75 × 150	< -15	< 0.1	(65 - 80)
[17]	5.15-5.85	24 × 28	< -16	< 0.15	> 60
[18]	5.6 - 5.9	54 × 30	< -20	< 0.05	= 45
[19]	4.03 - 5.4	105 × 50	< -27	< 0.05	(65 - 68)
This work	4.4-4.9 or 5.15-5.925	24 × 21	< -21	= 0	(56-67)

Conclusion

A mobile phone with a two-element antenna design was proposed for the use of LTE and 5G MIMO communications. This job involved the simulation and fabrication of a novel fractal MIMO antenna for the bands ranges of (4.4-4.9) GHz and (5.15-5.925) GHz. The different bands were controlled by way of the application of decoupling hybrid technique (neutralizationlines and defected ground structure). Besides enhancing the isolation between the antenna elements, the ECC between the signals received by the MIMO antenna ports was sufficiently reduced to meet the specifications for 5G applications.

Authors: *A. M. Ibrahim, Email: ayman971972@gmail.com; I. M. Ibrahim, Email: imranibrahim@utem.edu.my; N. A. Shairi, Email: noorazwan@utem.edu.my. The address for all authors Faculty of Electronics and Computer Engineering, Universiti Teknikal Malaysia Melaka (UTeM), 76100 Durian Tunggal, Melaka, Malaysia.*

REFERENCES

[1] A. M. Ibrahim, I. M. Ibrahim, and N. A. Shairi, "A compact quad bands-notched monopole antenna for ultra-wideband wireless communication," Religación, 2019. 53, (9), pp. 1689–1699.

[2] A. M. Ibrahim, I. M. Ibrahim, and N. A. Shairi, "Design a Compact Wide Bandwidth of a Printed Antenna using Defected Ground Structure," J. Adv. Res. Dyn. Control Syst, 2019, 11, (02), pp. 1065–1076, 2019.

[3] A. M. Ibrahim, I. M. Ibrahim, and N. A. Shairi, "Compact MIMO antenna with high isolation for 5G smartphone applications," J. Eng. Sci. Technol. Rev., 2019, 12, (6), pp. 121–125.

[4] H. Alsariera et al., "Compact CPW-fed broadband circularly polarized monopole antenna with inverted L-shaped strip and asymmetric ground plane," Prz. Elektrotechniczny, 2020, 96, (4), pp. 53–56.

[5] H. Alsariera, Z. Zakaria, and A. bin A. M. Isa, "New broadband L-shaped CPW-fed circularly polarized monopole antenna with asymmetric modified ground plane and a couple series-aligning inverted L-shaped strip," AEU - Int. J. Electron. Commun., 2020, 118, p. 153139.

[6] A. M. Ibrahim, I. M. Ibrahim, and N. A. Shair, "A Compact Sextuple Multi-Band Printed Monopole Antenna," Opcion, 2018, 86,(6), pp. 1448–1467.

[7] A. M. Ibrahim, I. M. Ibrahim, and N. A. Shairi, "Compact MIMO Slot Antenna of Dual-Bands for LTE and 5G Applications," Int. J. Adv. Sci. Technol., 2019, 28, (13), pp. 239–246.

[8] A. M. Ibrahim, I. M. Ibrahim, and N. A. Shairi, "Compact MIMO Slots Antenna Design with Different Bands and High Isolation for 5G Smartphone Applications," Baghdad Sci. J., 2019, 16, (4), pp. 1093–1102.

[9] H. Alsariera et al., "New CPW-fed Broadband Circularly Polarized Planar Monopole Antenna Based on a Couple of Linked Symmetric Square Patches," Int. J. Microw. Opt. Technol., 2020, 1, (2), pp. 95–103.

[10] A. M. Ibrahim, I. M. Ibrahim, and N. A. Shairi, "Compact MIMO Antenna for LTE and 5G Applications," Int. J. Microw. Opt. Technol., 2020,. 15(4), pp. 360-368, 2020.

[11] P. Shibi Kirubavathy and K. Ramprakash, "Design of Sierpinski Fractal Antenna for wideband applications,"2018,10(2) Int. Conf. Innov. Information, Embed. Commun. Syst. ICIIECS, pp. 1–4.

[12] A. T. Abed, M. S. Jit Singh, and M. T. Islam, "Compact Fractal Antenna Circularly Polarised Radiation For Wi-Fi And WiMAX Communications," IET Microwaves, Antennas Propag.,2018, 12(14), pp. 2218–2224.

[13] G. Das, R. K. Gangwar, and M. S. Sharawi, "Triple-port , two-mode based two element cylindrical dielectric resonator antenna for MIMO applications," Microw Opt Technol Lett, 2018,4 (60), pp. 1566–1573.

[14] R. Mark and S. Das, "Near Zero Parameter Metamaterial Inspired Superstrate for Isolation Improvement in MIMO Wireless Application," Frequenz, vol. 0, no. 0, 2019.

[15] N. L. Nguyen and V. Y. Vu, "Gain enhancement for MIMO antenna using metamaterial structure," Int. J. Microw. Wirel. Technol., 2019,4,(16), pp. 2–13.

[16] N. O. Parchin et al., "Eight-Element Dual-Polarized MIMO Slot Antenna System for 5G Smartphone Applications," IEEE Access, 2019, 7,(6), pp. 15612–15622.

[17] C. Y. Hsu, L. T. Hwang, F. S. Chang, S. M. Wang, and C. F. Liu, "Investigation of A Single-Plate Π-Shaped Multiple-Input-Multiple-Output Antenna with Enhanced Port Isolation for 5 Ghz Band Applications," IET Microwaves, Antennas Propag., 2016,10, (5), pp. 553–560.

[18] M. A. Abdalla and A. A. Ibrahim, "Simple μ-negative Half Mode CRLH Antenna Configuration for MIMO Applications," Radioengineering, vol. 26, no. 1, pp. 45–50, 2017.

[19] S. Chaudhuri, R. S. Kshetrimayum, and R. K. Sonkar, "High Inter-Port Isolation Dual Circularly Polarized Slot Antenna with Split-Ring Resonator Based Novel Metasurface," AEU - Int. J. Electron. Commun., 2019,107,(4), pp. 146–156.